

Near Optimal Flows in a Swirl Atomizer

L. Craig, N. Barlow, S.N. Patel, B. Kanya, and S.P. Lin*
Department of Mechanical and Aeronautical Engineering
Clarkson University, Potsdam, NY 13676

Abstract

Here we offer a new inviscid theory of swirl atomizers. It is mathematically demonstrated that for a given reservoir pressure, a maximum possible discharge rate may be achieved only when the air core radius at the outlet happens to be the critical radius predicted by the theory. At the critical radius, the swirl atomizer is operated at an ideal condition and the pressure required is the minimum possible for a given discharge rate. In practice, a swirl atomizer is never operating at an ideal condition. This is due to many factors including the neglected viscous dissipation. Even for inviscid fluids the operation may not be optimal, either because the nozzle is too short or too long. For the former case the liquid layer has not yet thinned to the critical thickness. For the latter case the liquid layer is thinned beyond the critical thickness. An efficiency coefficient is defined to characterize the off optimal condition. Based on inviscid theory a third order algebraic equation is derived for the air core radius. A closed form solution of this equation is obtained. Based on this solution, the air core radius and the spray angle are calculated as functions of the efficiency coefficient and geometric parameters. These include the swirl chamber radius and the inlet radius (in the unit of the outlet radius). The theoretical results are compared with the known experimental results and some results of numerical simulation. The comparisons reveal the extent of the deviation of the experimental swirl nozzle from the ideal atomizer. With these comparisons, we are able to deduce the effects of various factors on nozzle efficiency. The present theoretical results may be used as a target for design improvement, and as a bound for numerical simulation of swirl atomizers.

Introduction

As described in several books [1-3], swirl atomizers are used in fuel and chemical spraying and many other applications. The flow in a swirl atomizer can be depicted simply as follows. A pressurized liquid is fed tangentially from a small inlet into a chamber along its curved wall which is usually cylindrical. The liquid is accelerated both tangentially and axially as it is forced through a constricted region before exiting from a nozzle of inner radius r_o which is smaller than the chamber radius r_s , as depicted in Fig. 1. As the liquid accelerates, the pressure drops. When the pressure drops to the ambient air pressure an air-liquid interface is formed inside the nozzle. The atomization is initiated from the annular liquid layer of thickness $r_o - r_{ac}$, where r_{ac} is the inner radius of the annular layer at the nozzle outlet shown in Fig. 1. This figure is a reproduction of Fig.1 of Chinn [4]. It is desirable in practice to obtain the maximum possible flow rate for a given applied pressure. Various inviscid theories of the optimal flow which produces the maximum flow rate have been reviewed by Chinn [4]. He also compared known theoretical predictions of the optimal flow theories with known experimental results as well as the results of numerical simulations. The comparisons between theoretical, experimental, and numerical results are only qualitative at best. The predicted air core radius r_{ac} and the spray angles tend to be considerably larger than the experimental and numerical values. Lin [5] pointed out that the maximum flow rate is reached when the annular liquid layer at the outlet reaches the critical thickness at which the wave at the outlet starts to propagate upstream to slow down the flow. In experiments and numerical simulation, the optimal thickness is either not yet reached due to the nozzle being too short or the liquid is over accelerated to overshoot the critical condition. Here we offer a new inviscid theory which allows the nozzle to operate at off optimal condition. The theoretically predicted air core radii for various nozzle efficiencies are compared with the known experimental results and some results obtained with numerical simulators. The comparisons reveal the extent of deviation from the ideal swirl atomizers used by different experimentalists, as well as numerical simulators. With these comparisons, we are able to deduce the effects of various factors on nozzle efficiency. The present theoretical results may be used as a guide and a target for design improvement and as a bound for numerical simulation of swirl atomizers using viscous fluids.

*Corresponding Author

Optimal Flow

Consider the flow in the swirl atomizer depicted in Fig. 1. A pressurized liquid enters through an inlet of radius r_i , into a chamber of radius r_s . The liquid enters tangentially with velocity w_i . The pressure difference between the inlet and outlet accelerates the liquid axially toward the nozzle of radius r_o . As the chamber is constricted, the liquid swirl is intensified, and the pressure is dropped. This allows an axisymmetric air core to be created when the pressure drop is sufficient. The air core geometry depends on the properties of the liquid; the inlet liquid pressure and the geometry of the nozzle. For a given applied liquid pressure and geometry of the atomizer, an inviscid liquid will yield the maximum discharge rate, which is equal to the atomization rate. This maximum discharge rate of the inviscid liquid may be raised if the atomizer geometry is changed. However, there is a limit to which the discharge can be raised, as explained below.

First, we will prove that for a given applied pressure, there exists an optimal air core radius for which the discharge rate is the maximum. Next, we will prove that for a given discharge, the pressure required for atomization is at its minimum when the optimal air core radius is reached at its outlet. In practice, the atomizer is never optimal. The theory of a non-optimal atomizer will be given in the next section.

Along the liquid-air core interface, the Bernoulli equation is

$$(u^2 + w^2)/2 + p/\rho = \Delta p/\rho, \quad (1)$$

where u and w are axial and tangential velocity respectively in the cylindrical coordinate system (r, θ, x) as shown in Fig. 1. The parameters p and Δp are the air pressure and the pressure at the inlet respectively, and ρ is the liquid density. Note that the radial component of the liquid velocity at the interface is small compared with the other two components, and thus is neglected in Eq. (1). The average inlet velocity, w_i , is $Q/(\pi r_i^2)$. Where Q and r_i being respectively the liquid discharge rate and the radius of the circular inlet. The angular momentum is conserved in the frictionless fluid and thus $wr = \text{constant}$. This constant may be identified with the angular momentum, $w_i(r_s - r_i)$, introduced at the inlet, where r_s is the maximum radius of the swirl chamber. Thus, we have

$$w = w_i(r_s - r_i)/r, \quad (2)$$

At the outlet, the axial velocity is equal to $Q/[\pi(r_o^2 - r_a^2)]$, r_a being the air core radius. Substituting this velocity and Eq. (2) into Eq. (1) we have

$$Q^2/[\pi(r_o^2 - r_a^2)]^2 + Q^2(r_s - r_i)^2/(\pi r_i^2 r_a^2) = 2\Delta p/\rho, \quad (3)$$

Note that the air pressure is put to zero and thus, Δp is now the supplied gauge pressure. In dimensionless form Eq. (3) is written as

$$1/(1 - R^2)^2 + 1/K^2 R^2 = 2\Delta p \pi^2 r_o^4 / \rho Q^2 = 1/C_D^2, \quad (4)$$

where the discharge coefficient

$$C_D^2 = \rho Q^2 / (2\Delta p \pi^2 r_o^4), \quad K = R_i^2 / (R_s - R_i), \quad (5)$$

and

$$R_i = r_i / r_o, \quad R_s = r_s / r_o, \quad R_a = r_a / r_o. \quad (6)$$

As pointed out by Lin [5], the discharge Q and applied pressure Δp must be treated as independent variables. For a given Δp there is an optimal R which yields the maximum Q . The maximum or minimum of Q can be obtained by finding the R for which $\partial Q / \partial R = 0$. To ascertain that the obtained R indeed yields maximum Q , we must have

$\partial^2 Q / \partial^2 R < 0$. The first derivative of Eq. (4) with respect to R gives

$$\frac{4R}{(1 - R^2)^3} - \frac{2}{K^2 R^3} = -\frac{4\pi^2 r_o^4 \Delta p}{\rho Q^3} \frac{\partial Q}{\partial R}. \quad (7)$$

Putting $\partial Q / \partial R = 0$ in Eq. (7), we obtain the equation which determines the critical radius $R = R_c = r_{ac} / r_o$,

$$4R_c / (1 - R_c^2)^3 - 2 / K^2 R_c^3 = 0. \quad (8)$$

To determine if R_c given by Eq. (8), indeed yields the maximum Q , we differentiate Eq. (7) once again with respect to R .

$$\frac{24R^2}{(1-R^2)^4} + \frac{4}{(1-R^2)^3} + \frac{6}{K^2R^4} = -\frac{4\pi^2r_o^4\Delta p}{\rho Q^3} \frac{\partial^2 Q}{\partial R^2} + \frac{12\pi^2r_o^4\Delta p}{\rho Q^4} \left(\frac{\partial Q}{\partial r} \right)^2. \quad (9)$$

At $R=R_c$, $(\partial Q / \partial R)$ in Eq. (9) is zero, and the coefficient of $(\partial^2 Q / \partial R^2)$ is negative, thus the left side of Eq. (9) is always positive, since $R < 1$. Therefore, $\partial^2 Q / \partial R^2 < 0$ at $R=R_c$. Hence, $R=R_c$ obtained from Eq. (8) indeed gives the maximum Q for a given Δp .

On the other hand, for a given Q , R_c gives the minimum Δp required as shown below. For a given constant Q , the first and second derivatives of Eq. (4) with respect to R give

$$\frac{4\pi^2r_o^4}{\rho Q^2} \frac{\partial(\Delta p)}{\partial R} = \frac{4R}{(1-R^2)^3} - \frac{2}{K^2R^3}, \quad (10)$$

and

$$\frac{4\pi^2r_o^4}{\rho Q^2} \frac{\partial^2(\Delta p)}{\partial R^2} = \frac{24R^2}{(1-R^2)^4} + \frac{4}{(1-R^2)^3} + \frac{6}{K^2R^4}. \quad (11)$$

The right side of Eq. (10) is zero at $R = R_c$ by virtue of Eq. (8). Hence $\partial \Delta p / \partial R = 0$ at $R = R_c$. Moreover, the right side of Eq. (11) is always positive, since $R < 1$; and the coefficient of $\partial^2(\Delta p) / \partial R^2$ is always positive. Hence, $\partial^2(\Delta p) / \partial R^2 > 0$ at $R = R_c$. Therefore, for a given Q , the pressure required is the minimum possible if the design of the nozzle allows the air-core radius to attain R_c at the outlet. The discharge coefficient, C_{DC} , corresponding to the optimal flow is obtained from Eq. (4), putting $R=R_c$, we get

$$C_{Dc}^2 = \frac{K^2 X_c (1 - X_c)^2}{K^2 X_c + (1 - X_c)^2}, \quad (12)$$

where $X_c = R_c^2$.

Non-Optimal Flows

The flow in a real swirl atomizer is never optimal even if the fluid is frictionless. The air-core radius must attain the optimal radius R_c even for an ideal fluid. If the optimal radius is not attained, the discharge rate will be smaller than the maximum possible, and the actual discharge coefficient C_{Da} will be less than C_{DC} . We characterize the actual atomizer with an efficiency coefficient, e , relating C_{DC} with C_{Da} . This is shown by

$$C_{Da} = e C_{DC}, \quad (13)$$

If $e=1$, the flow is optimal, and $e < 1$ gives the fraction of the optimal discharge. The corresponding dimensionless air-core radius is still governed by the dimensionless Bernoulli equation (4), except C_D is now replaced by $C_{Da}=eC_{DC}$ and R by the actual outlet radius $R_a=r_a/r_o$,

$$\frac{1}{(1-R_a^2)^2} + \frac{1}{K^2 R_a^2} = \frac{1}{e C_{DC}^2} \quad (14)$$

Eq. (14) can be written in terms of $X_a = R_a^2$ as

$$K^2 X_a^3 - X_a^2 (e C_{DC}^2 + 2K^2) - X_a (e C_{DC}^2 K^2 - 2e C_{DC}^2 - K^2) - e C_{DC}^2 = 0 \quad (15)$$

This third order algebraic equation can be solved easily for X_a . The positive square root X_a gives R_a . The calculated R_a for different e , K , and C_{Da} are compared with the known experiments and numerical simulation results in the next section.

The spray angles from the non-optimal nozzle can be calculated with minor modification of the known methods described by Chinn [4]. The details of derivation will not be given here due to space limitations. From a kinematic consideration at the nozzle outlet, the half-spray angle α between the nozzle axis and the liquid trajectory at R_a is given by (c.f. Eq. (146) of Chinn [4])

$$\sin \alpha = w_a / (w_a^2 + u_a^2)^{1/2} = C_{Da} / K R_a \quad (16)$$

and the half-angle to the liquid trajectory leaving the nozzle inner wall β is given by (c.f. Eq. (149) of Chinn [4])

$$\sin \beta = C_{Da} / K. \quad (17)$$

Following G.I. Taylor's [6] method, which considers the dynamical effects of the liquid leaving the nozzle, we find the spray angle at R_a to be governed by (c. f. Eq. (133) of Chinn [5]).

$$\cos \alpha_T = \frac{1 - R_a^2}{2C_{Da}} + \frac{C_{Da}}{2(1 - R_a^2)} + \frac{C_{Da}}{K^2} \ln R_a \quad (18)$$

Results and Discussion

The solution of Eq. (14) for the optimal case with $e=1$ has only two real roots for R_a ; one is positive and the other negative. The negative radius does not have physical meaning. The positive root of $R_a=R_c$ for $e=1$ is plotted against K as the dashed line in Fig. 2. For the values of e other than one, Eq. (14) has two positive real R_a , one is larger and the other is smaller than R_c . R_a as a function of K for different nozzle efficiencies are plotted in the same figure. It is seen that the efficiency of the experimental nozzles and the nozzle simulated numerically ranges from 0.4 to 0.8, indicating that the nozzles have some room for improvement. Some experimental points included the value of $N=r_o/r_s$ in addition to K . However, these experimental points were obtained in the range of $K<1$. To better elucidate the effect of N on the nozzle efficiency, the results in the region of small k of Fig. 2 is enlarged in Fig. 3. Some experimental results with higher efficiencies, which were not included in Fig. 2, are also added in this figure. It is seen that as N is increased the curve tends to move toward the highest efficiency curve that of $e=1$. It appears that a smaller nozzle inner radius relative to the swirl chamber radius tends to improve the efficiency.

The results on the spray angles, as well as more extensive results explaining the effects of nozzle geometry on the nozzle efficiency, will be submitted to Atomization and Sprays. If time permits, some additional results will be presented at the conference.

Nomenclature

C_D	discharge coefficient
e	discharge efficiency
K	a geometric parameter
N	r_o/r_s
p	pressure
Δp	applied liquid pressure
Q	discharge
r	dimensionless radius
R	dimensional radius
u	axial velocity
w	tangential velocity
x	axial distance
α	spray angle from air core radius
β	spray angle from nozzle wall
ρ	density

Subscripts

a	actual condition
c	critical condition
i	inlet
o	outlet
s	swirl chamber

References

1. Lefebvre, H., *Atomization and Sprays*, Hemisphere, Bristol, Pa. (1989).
2. Bayvel, L. and Orzechowski, Z., *Liquid Atomization*, Taylor and Francis, New York (1993).

3. Khavkin, Y. I., *The Theory and Practice of Swirl Atomizers*, Taylor and Francis, New York (2003).
4. Chinn, J. J. *Atomization and Sprays*, vol. 19, 263 – 308 (2009).
5. Lin, S.P., *Atomization and Sprays*, vol. 19, 309-310 (2009).
6. Taylor, G. I., *Q. J. Mech. Appl. Math.*, 3, 129-139 (1950).
7. Datta, A. and Som, S. K. *Int. J. Heat Fluid Flow*, 21, 412-419 (2000).
8. Halder, M. R., Dash, S. K. and Som, S. K., *Thermal Fluid Sci.*, 26, 871-878 (2002).
9. Kutty, P. S., Narasimhan, M. V. and Narayanaswamy, K., Tokyo, pp. 93-100, First International Conference on Liquid Atomization and Spray Systems, July 1978.
10. Wang, D. and Ma, Z., pp.99-2401/ AIAA/ ASME/ SAE/ ASEE Joint Propulsion Conf. Exhibit, AIAA, 1999.
11. Hansen K. G. and Madsen, J. A Computational and Experimental Study of the Internal Flow in a scaled pressure Swirl Atomizer, M.sc. thesis, Alborg University Esbjerg, 2001.
12. De Keuklaere, H. J. K., The Internal Flow of a Swirl Atomizer Nozzle, M.Sc. thesis Department of Mechanical Engineering University of Manchester (UMIST),1995.

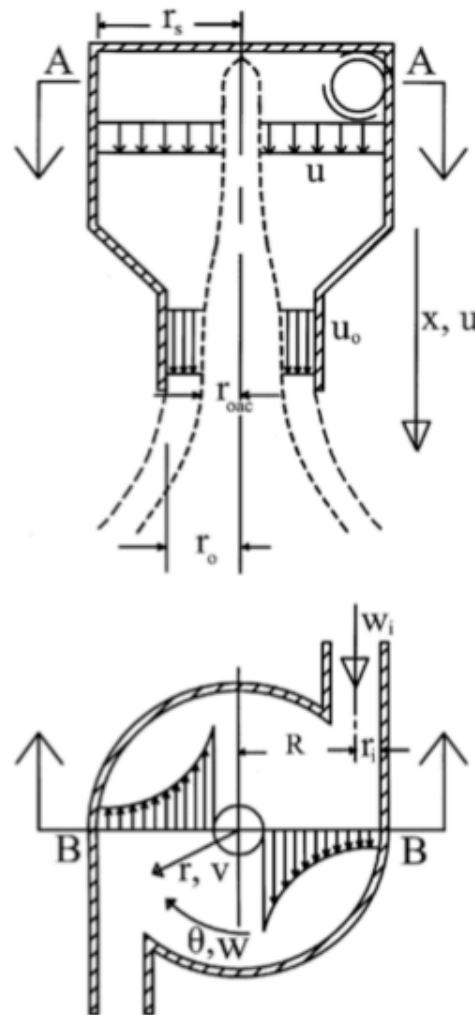


Figure 1: The simplified flow in a diagrammatic representation of a two-inlet swirl atomizer, showing nomenclature and cylindrical coordinate conventions.

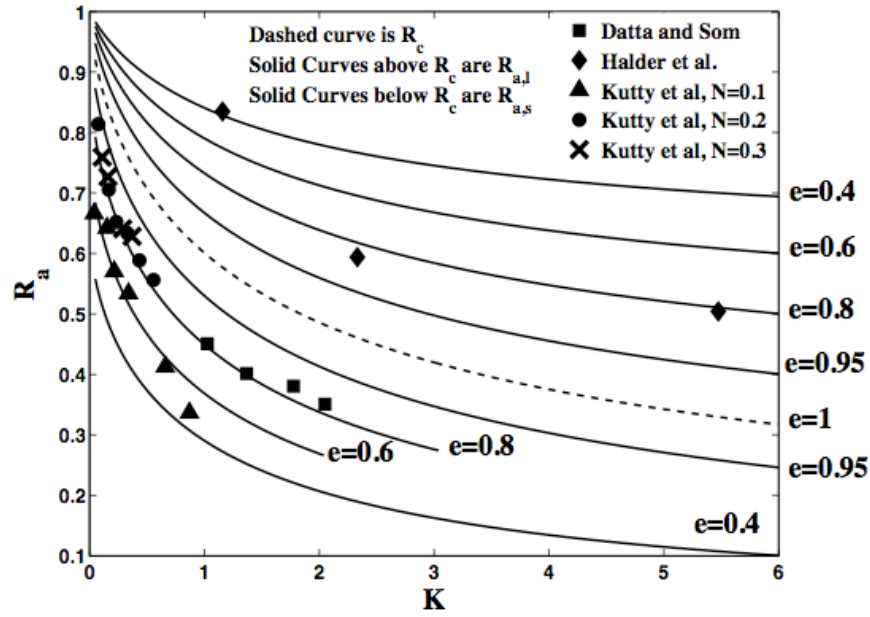


Figure 2: $R_{a,i}$, $R_{a,s}$, and R_c plotted against k for different values of e , in comparison with the numerical results of Datta and Som [1] (■), the experimental results of Halder et al [8] (◆), and the experimental results of Kutty et al [9]: for $N=0.1$ (▲), $N=0.2$ (●), and $N=0.3$ (×).

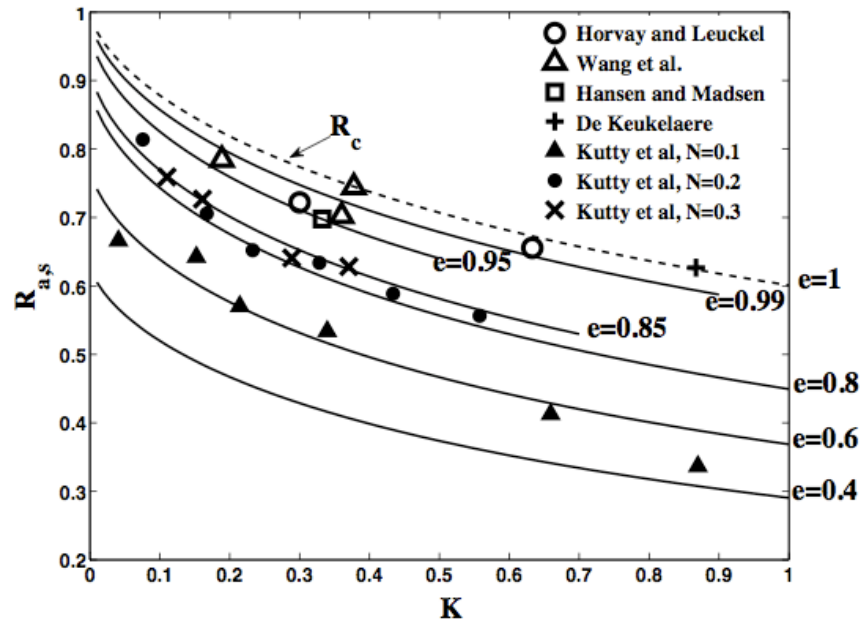


Figure 3: $R_{a,s}$ and R_c plotted against k for different values of e , in comparison with the experimental points of Horvay and Lueckel (○) [10], Wang et al. (Δ) [10], Hansen and Madsen (□) [11], De Keukelaere [12] (+), and Kutty et al [9]: for $N=0.1$ (▲), $N=0.2$ (●), and $N=0.3$ (×).